The high-frequency oscillation in systems with Rayleigh damping model

Junjie Xu[1], Yuli Huang[2], Zhe Qu[3]

[1] Associate Professor, Key Laboratory of Earthquake Engineering and Engineering Vibration, Institute of Engineering Mechanics, China Earthquake Administration, Harbin, Heilongjiang, China.
[2] Senior Analyst, Arup, San Francisco, CA, USA.
[3] Professor, Key Laboratory of Earthquake Engineering and Engineering Vibration, Institute of Engineering Mechanics, China Earthquake Administration, Harbin, Heilongjiang, China.

ABSTRACT

Rayleigh damping model suggests high physical damping at high frequency. This is considered to be desirable to filter the inaccurate high-frequency responses in numerical transient analysis. However, with some widely adopted time integrators, the simulated system shows unexpected oscillation as if no damping is in effect. This paper presents an investigation on such observation and offers an insightful explanation. Following the linear stability analysis approach, the eigenvalues of the amplification matrix corresponding to an integrator are derived in terms of physical damping ratio and dimensionless frequency. It is concluded that oscillation and the associated small algorithmic damping effect is attributed to an asymptotic eigenvalue of -1, with illustration using Newmark trapezoidal integrator.

Keywords: High-frequency oscillation; Rayleigh damping; Trapezoidal rule; Eigenvalues of amplification matrix.

1 INTRODUCTION

If a structural system is discretized in space, the following semi-discrete equations of motion can be obtained.

$$\mathbf{M\ddot{u}} + \mathbf{C\dot{u}} + \mathbf{Ku} = \mathbf{F} \tag{1}$$

where, **M**, **C**, **K** and **F** are the mass, damping, stiffness matrices and the external load vector, and $\mathbf{u}$, $\dot{\mathbf{u}}$ and $\ddot{\mathbf{u}}$ denote displacement, velocity and acceleration respectively. Direct time integration is probably the most generic way to solve the equations of motion and implicit schemes are mostly preferred for structural dynamics. Many implicit schemes have been developed, such as the Newmark method[2], the HHT-α method [3], the three parameters method (generalized-α method) [4],[5], and the Bathe's method[6][7][8].

In many structural dynamics applications only lower frequency response is of interest, and the higher frequency response of the discretized system generally do not accurately represent the behavior of the original problem. It is often desirable to remove any spurious participation of the higher modes in the transient analysis [3]. This is particularly important when solving problems exhibiting nonlinear material behavior, e.g. plasticity. For such problems, spurious oscillations would feed into the constitutive routines and adversely affect the computational performance [9].

In order to filter high-frequency response, one way is to use an algorithm with high-frequency dissipation characteristics, such as the algorithms mentioned above [3]-[7]. Another point of view is that the use of Rayleigh damping can naturally filter out high-frequency response. For the Rayleigh damped system, because a high-frequency response theoretically corresponds to high physical damping, it is widely considered to be helpful in damping out spurious high-frequency response in the system. However, this may not be the case, e.g. when the Newmark trapezoidal rule is applied to calculate the large-scale structural dynamic problems with Rayleigh damping, the high-frequency oscillation persists. Hughes pointed out the problem after studying the spectral radius of the amplification matrix in his work [10].

In this paper, the counterintuitive fact that Rayleigh damping cannot effectively filter the high-frequency oscillation of the system is demonstrated via three typical examples. The eigenvalues of the amplification matrix of the trapezoidal rule are studied in detail. An alternative explanation for the cause of oscillation is presented.

2 OSCILLATION OF OVERDAMPED SYSTEMS

2.1 Rayleigh damping model

In structural dynamic analysis problems, Rayleigh damping [1] is one of the most common damping models. For Rayleigh damping, the **C** matrix is derived from a combination of the mass matrix and the stiffness matrix

$$\mathbf{C} = \alpha\mathbf{M} + \beta\mathbf{K} \tag{2}$$

α and β are determined by two given frequency values ω_i and ω_j and corresponding damping ratio ξ_i and ξ_j. In general, $\xi = \xi_i = \xi_j$. As is shown in Fig.1, Rayleigh damping is characterized by a frequency within the frequency range (ω_i, ω_j) of the structure, the damping ratio is a bit smaller than ξ. However, since the damping corresponding to the high frequency is approximately proportional to the natural frequency ω_n, when the structure contains relatively stiff parts or the finite element mesh contains elements with very small size, the highest frequency of the structure is very large, and the corresponding damping ratio is also very large. Therefore, if the modes of the structure are decomposed, the system corresponding to the high-frequency mode is overdamped.

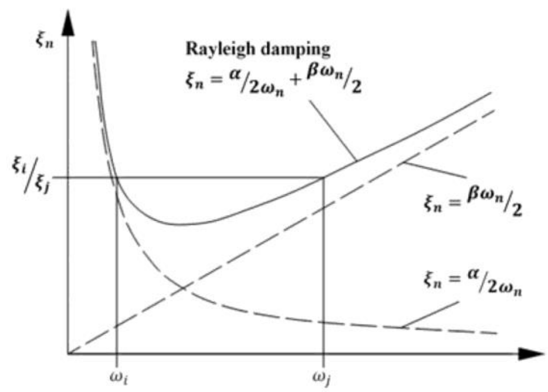

Fig.1 Rayleigh damping model

2.2 Single DOF Overdamped System and the exact solution

For the purposes of investigation, it is advantageous to reduce the coupled equations of motion in Eq.(1) and the algorithmic equations to a series of uncoupled single-degree-of-freedom systems. The equation of motion associated with the individual mode is

$$\ddot{u} + 2\xi\omega\dot{u} + \omega^2 u = f \tag{3}$$

and the initial conditions are $u(0)=u_0$ and $\dot{u}(0) = v_0$. Only free vibration case (f=0) is studied in this paper. There are three cases for the exact solution of Eq.(3) [10]. If ξ>1, the system is overdamped and the exact solution is

$$u(t) = \mathrm{e}^{-\xi\omega t}\left(u_0 \cosh \omega_E t + \frac{v_0 + \xi\omega u_0}{\omega_E} \sinh \omega_E t \right) \tag{4}$$

where, $\omega_E = \omega\sqrt{\xi^2 - 1}$. For overdamped systems, vibration (or oscillation) does not occur.

2.3 Oscillation response of trapezoidal rule

To calculate the dynamic response of a system defined by Eq.(3), methods of direct time integration are commonly used, among which, the Newmark method[2] with two parameters of 1/2 and 1/4, also known as trapezoidal rule or constant acceleration method, is often used. Although this method is most commonly used, when the method is applied to structural dynamic analysis, even if Rayleigh damping is used to make the high-frequency component overdamped, the high-frequency response still exists. The following three examples will illustrate this counterintuitive phenomenon.

Example 1 : SDOF system.

The parameters in Eq.(3) are

$$\xi = 250 \quad \omega = 10000 \quad f = 0 \tag{5}$$

with the initial conditions of u_0=1 and v_0=1. It is an overdamped system. The system was analyzed using the Newmark method, and the size of the time step was set to be Δt=0.01. The comparison of the solutions of the Newmark method and the exact solution shown in Eq.(4) is shown in the Fig.2.

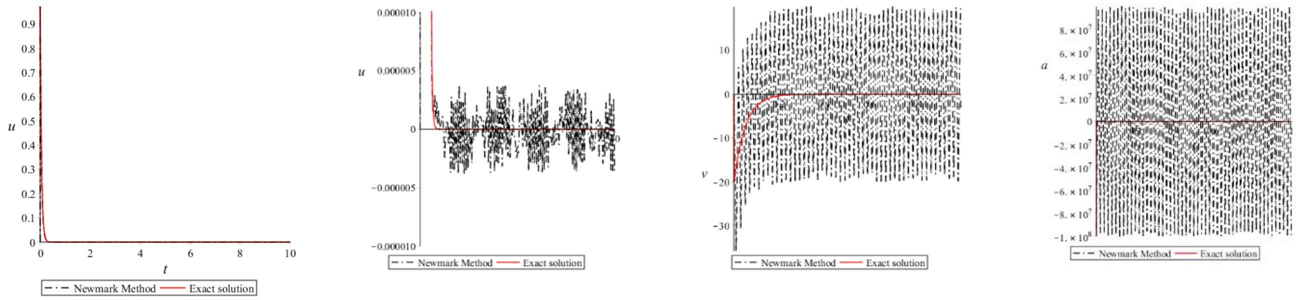

(a) Displacement *(b) Displacement (zoomin)* *(c) Velocity* *(d) Acceleration*

Fig.2 Comparison of numerical and exact solutions

Example 2: MDOF system [8]

An MDOF spring system shown in Fig.3 was considered. Bathe adopted this example to verify that his algorithm is superior to the Newmark method in solving the stiff problems.

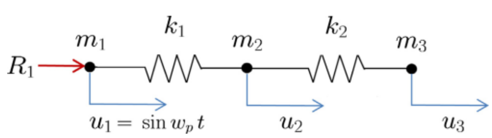

Fig.3 Model problem of a MDOF spring system

The matrices of the governing equations shown in (1) are

$$\mathbf{M} = \begin{bmatrix} m_2 & 0 \\ 0 & m_3 \end{bmatrix} \quad \mathbf{K} = \begin{bmatrix} k_1 + k_2 & -k_2 \\ -k_2 & k_2 \end{bmatrix} \quad \mathbf{F} = \begin{Bmatrix} k_1 u_1 \\ 0 \end{Bmatrix} \tag{6}$$

with k_1=10^8, k_2=1, m_1=0, m_2=1, m_3=1, ω_p=1.2. The two frequencies ω_1 and ω_2 of the system are 1 and 10^4, respectively. The Rayleigh damping matrix **C** is calculated by Eq.(2), and the parameter is selected as α = 0.05, β = 0.05, such that the physical damping ratios of the two modes are ξ_1 =0.05 and ξ_2 =250. This example represents the stiff and flexible parts of a much more complex structural system. The left high stiffness spring in the model problem is used to represent almost rigid connections or penalty factors used, while the right flexible spring represents the flexible parts of the complex structural model. The existence of such a nearly rigid part is likely to cause the result of oscillation.

For comparison, the trapezoidal rule and the Bathe's algorithm were used for calculation of this problem. The step size is Δt=0.01. The results are shown in Fig.4. For the Newmark method, high-frequency oscillations occur again for the acceleration.

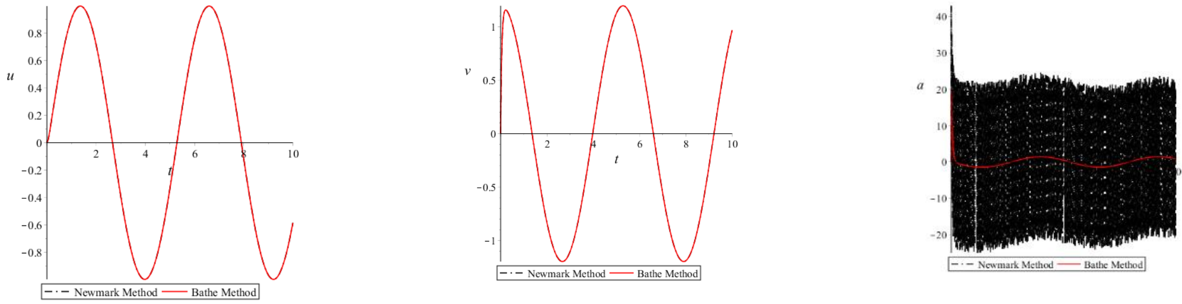

(a) Displacement of m_2 *(b) Velocity of m_2* *(c) Acceleration of m_2*

Fig.4 Comparison of Newmark method and Bathe's method for response of 2nd DOF

Example 3: Distortion of shear force response adjacent to very rigid parts in a frame structure

The model in Fig.5 is a two-story space frame subjected to ground motion of 1940 El Centro NS record at the base. The material properties and dimensions of the model are listed in Fig.5(a), where E is Young' modulus, μ is Poisson's ratio, ρ_b and ρ_c are respectively the density of beams and columns, b, h and L are respectively the width, depth, length of every column/beam. Euler-Bernoulli beam elements are used to mesh the beams and columns in the frame. Model A in Fig.5(a) represents an ordinary meshing strategy, in which a beam/column component is represented by one beam element. Model B is established for the purpose of comparison, in which a very short element with a length of half the beam width, 0.5b, is inserted on top of each column at the first story (Fig.5(b)). Meanwhile, the Young's Modulus of the short element is 5000 times E to simulate the rigid zone of the beam-column joint.

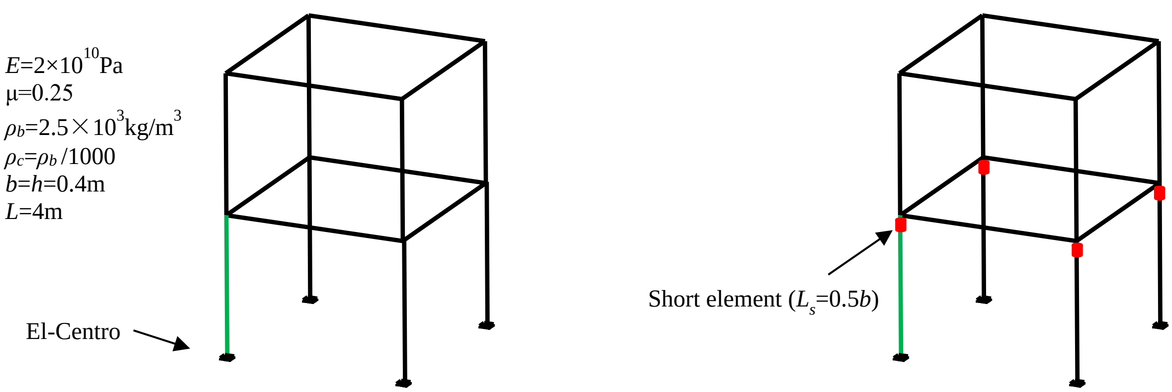

(a) Model A *(b) Model B*

Fig.5 A frame structure

A lumped mass matrix generated by the HRZ[11] method is adopted. Rayleigh damping is involved with a damping ratio of 0.05. The first three angular frequencies of this structure are ω_1 = 30.6 rad/s, ω_2 = 30.6 rad/s, ω_3 = 44.2 rad/s. The two coefficients of Rayleigh damping are α = 1.808, β = 0.001337, which are determined by the first and third angular frequencies. For comparison, the following three cases of analysis were implemented. The time step is set to be 0.01s for the analysis.

Case a) Model A by *trapezoidal rule*;

Case b) Model B by *trapezoidal rule*;

Case c) Model B by Bathe's method.

The time history responses of the shear force at top of one column of the first story (the green column in Fig.5) are compared in Fig.6.

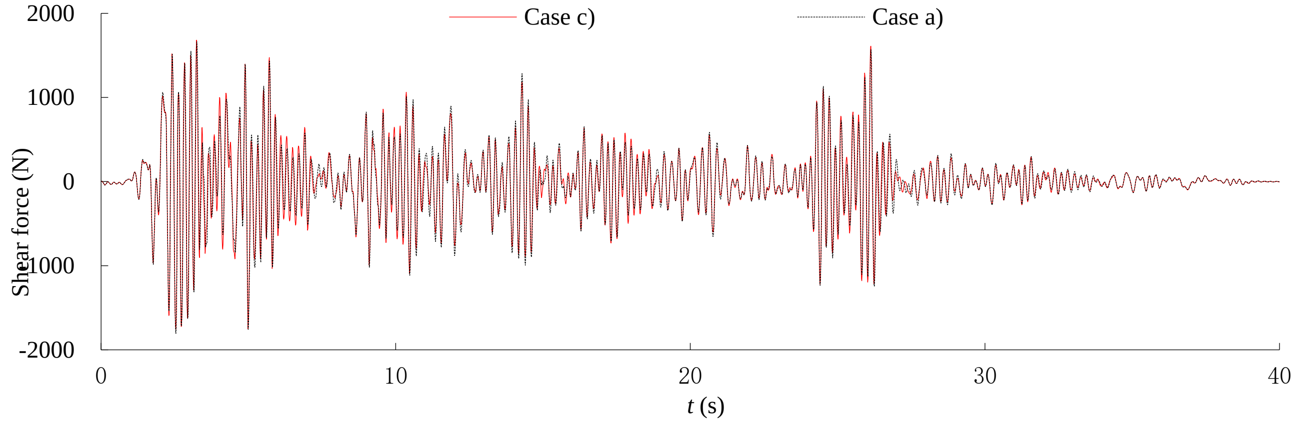

Fig.6a Comparison of Case(a) and Case(c)

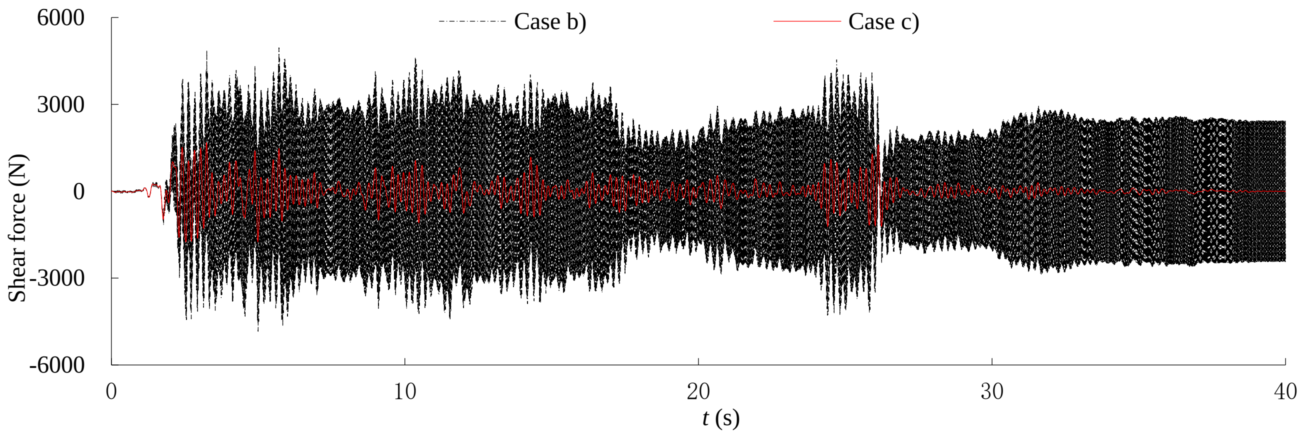

Fig.6b Comparison of Case(b) and Case(c)

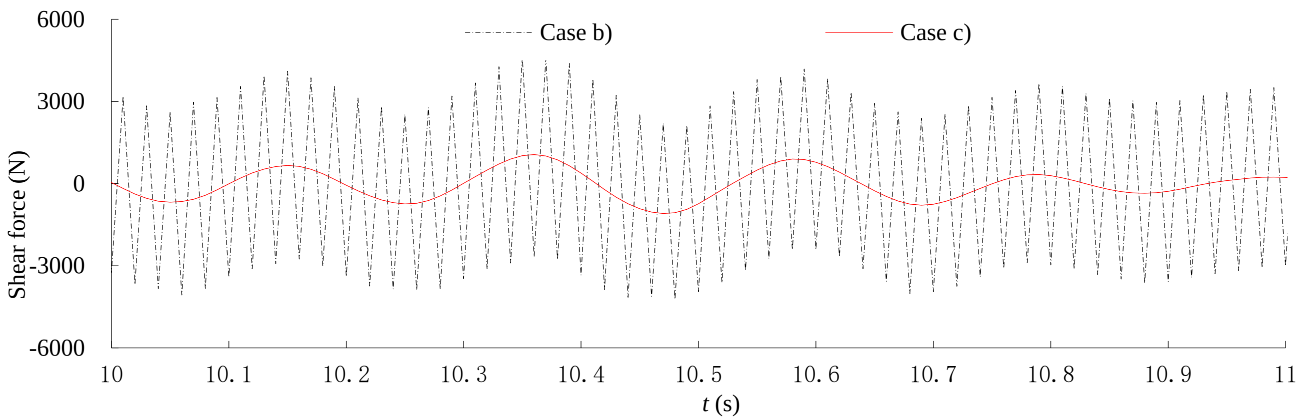

Fig.6c Comparison of Case(b) and Case(c) (zoomin)

Remarks

In the Rayleigh-damped system, if there are very rigid parts in the system, the dynamic response of the degree of freedom adjacent to these parts exhibits strong oscillation if trapezoidal rule is applied. The Bathe's algorithm can effectively eliminate these high-frequency oscillations and can be used as a reference solution.

3 AN ALTERNATIVE EXPLANATION FOR THE CAUSE OF OSCILLATION

In order to study the causes of the high-frequency oscillation of the trapezoidal rule, the eigenvalues of the amplification matrix of the trapezoidal rule are studied in this section.

The recursive format of trapezoidal rule [12] is

$$\mathbf{Y}_i = \mathbf{A}^{Trape}\mathbf{Y}_{i-1} \tag{7}$$

where, $\mathbf{Y}_{i-1}$ and $\mathbf{Y}_i$ are vectors of the displacement, velocity and acceleration at the start time and the end time of the *i*-th time step respectively.

$$\mathbf{Y}_{i-1} = \begin{Bmatrix} u_{i-1} \\ \Delta t \cdot v_{i-1} \\ \Delta t^2 \cdot a_{i-1} \end{Bmatrix} \quad \mathbf{Y}_i = \begin{Bmatrix} u_i \\ \Delta t \cdot v_i \\ \Delta t^2 \cdot a_i \end{Bmatrix} \tag{8}$$

and $\mathbf{A}^{Trape}$ is the amplification matrix of trapezoidal rule, of which the expression with respect to ξ and Ω is

$$\mathbf{A}^{Trape} = \begin{bmatrix} \frac{4(\Omega\xi+1)}{\Omega^2+4\Omega\xi+4} & \frac{2(\Omega\xi+2)}{\Omega^2+4\Omega\xi+4} & \frac{1}{\Omega^2+4\Omega\xi+4} \\ -\frac{2\Omega^2}{\Omega^2+4\Omega\xi+4} & -\frac{\Omega^2-4}{\Omega^2+4\Omega\xi+4} & \frac{2}{\Omega^2+4\Omega\xi+4} \\ -\frac{4\Omega^2}{\Omega^2+4\Omega\xi+4} & -\frac{4\Omega(\Omega+2\xi)}{\Omega^2+4\Omega\xi+4} & -\frac{\Omega(\Omega+4\xi)}{\Omega^2+4\Omega\xi+4} \end{bmatrix} \tag{9}$$

where Ω represents the dimensionless frequency with the expression

$$\Omega = \omega\Delta t \tag{10}$$

The eigenvalues of $\mathbf{A}^{Trape}$ are given by

$$\lambda_{1,2} = A_1 \pm \sqrt{A_1^2 - A_2} \quad \text{and} \quad \lambda_3 = 0 \tag{11}$$

where

$$A_1 = \frac{4-\Omega^2}{\Omega^2+4\Omega\xi+4} \quad A_1^2 - A_2 = \frac{16\Omega^2\left(\xi^2-1\right)}{\left(\Omega^2+4\Omega\xi+4\right)^2} \tag{12}$$

For the overdamped system, i.e. $\xi > 1$, $\lambda_{1,2}$ shown in Eq.(11) are two real values.

For comparison with the trapezoidal rule, the amplification matrix and corresponding eigenvalues of the exact solution, which can be calculated by Eq.(4), are also given as follows.

$$\mathbf{A}^E = e^{-\xi\Omega}\begin{bmatrix} \cosh(\Omega_E) + \frac{\xi\Omega}{\Omega_E}\sinh(\Omega_E) & \frac{1}{\Omega_E}\sinh(\Omega_E) \\ -\frac{\Omega^2}{\Omega_E}\sinh(\Omega_E) & \cosh(\Omega_E) - \frac{\xi\Omega}{\Omega_E}\sinh(\Omega_E) \end{bmatrix} \tag{13}$$

where

$$\Omega_E = \omega_E \Delta t \quad \omega_E = \omega\sqrt{\xi^2 - 1} \tag{14}$$

Since the acceleration does not appear in the recurrence formula, the dimension of A is 2 by 2. The eigenvalues of $\mathbf{A}^E$ are

$$\lambda_{1,2}^E = \mathrm{e}^{-\xi\Omega}\left(\cosh\left(\Omega_E\right) \pm \sinh\left(\Omega_E\right)\right) \tag{15}$$

which are also two real values.

The comparison of eigenvalues between the trapezoidal rule and the exact solution is illustrated in Fig.7.

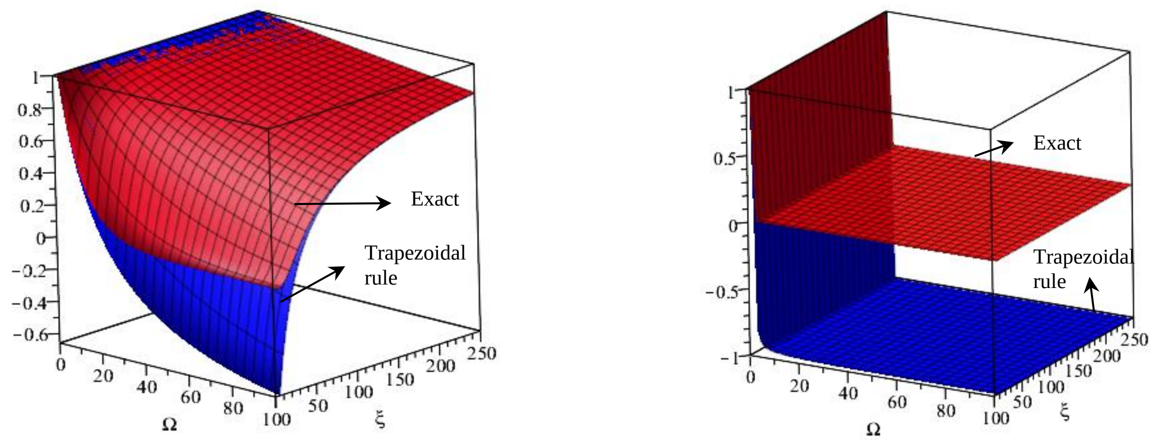

(a) λ_1 (b) λ_2

Fig.7 Comparison of the two eigenvalues between trapezoidal rule and the exact solution

The relationship between the displacement response and the eigenvalues can be expressed by[10]

$$u_i = u\left(n \cdot \Delta t\right) = c_1\lambda_1^n + c_2\lambda_2^n \tag{16}$$

At high frequencies and high damping, the second eigenvalue λ_2 approaches -1(for example, when Ω=100 and ξ=250, λ_1 = 0.81818 and λ_2 = -0.99992). The second term at the right-hand-side of Eq.(16) is approximately equal to $c_2(-1)^n$, of which the sign will switch every time step, and the value almost does not decay, causing the "saw-tooth" oscillations of the response, as is shown in Fig.2, Fig.4 and Fig.6. While for the exact solution, the second eigenvalue λ_2 tends to zero with increasing frequency and damping, which is why the exact solution does not oscillate.

4 CONCLUSIONS

Rayleigh damping is the most commonly used damping model in structural dynamic analysis. At the same time, the trapezoidal rule is also the most commonly used integral algorithm in structural dynamic analysis. However, when the two are combined, the high-frequency oscillation occurs counter-intuitively, resulting in serious distortion of the dynamic response.

Aiming at this problem, an alternative explanation for the cause of oscillation is presented in this paper. Taking the Newmark trapezoidal rule as an example, the eigenvalues of the amplification matrix of the algorithm are expressed as a function of the physical damping ratio ξ and the dimensionless frequency Ω. It is found that with the increase of ξ and Ω, one of the eigenvalues tends to -1, which is directly causing oscillation. Therefore, the cause for the fact that the Rayleigh damping model is difficult to damp out the high-frequency response is alternatively explained.

To avoid the high-frequency oscillation, two methods can be used. One is to use an integral method with considerable numerical dissipation, such as Bathe's method [6]. Secondly, rather than the Rayleigh damping model, a frequency-insensitive damping model can be adopted, such as the damping model[13] proposed by Huang et al., which gives nearly equal physical damping for any order frequency, and thus avoids high-frequency oscillation caused by the overdamped case.

ACKNOWLEDGMENTS

Acknowledge the sources of support by Scientific Research Fund of Institute of Engineering Mechanics, China Earthquake Administration (Grant No. 2016A05 and 2017B03).

REFERENCES

[1] Strutt, J. W., & Rayleigh, B. (1945). The theory of sound. Dover.

[2] Newmark, N.M. (1959). A method of computation for structural dynamics. *Journal of the Engineering Mechanics* Division, 85(3), 67–94.

[3] Hilber, H. M. , Hughes, T. J. R. , & Taylor, R. L. (1977). Improved numerical dissipation for time integration algorithms in structural dynamics. *Earthquake Engineering & Structural Dynamics*, 5(3), 283-292.

[4] Shao H.P., Cai C.W. (1988).The direct integration three-parameter optimal schemes for structural dynamics. *In: Proceedings of the international conference: machine dynamics and engineering applications. Xi'an Jiaotong University Press;* p. C16–20.

[5] Chung, J. , & Hulbert, G. M. (1993). A time integration algorithm for structural dynamics with improved numerical dissipation: the generalized-alpha method. *Journal of Applied Mechanics*, 60(2), 371.

[6] Bathe K. J. , Baig, M. M. I. (2005). On a composite implicit time integration procedure for nonlinear dynamics. *Computers & Structures*, 83(31-32), 2513-2524.

[7] Bathe K. J. (2007). Conserving energy and momentum in nonlinear dynamics: a simple implicit time integration scheme. *Computers & Structures*, 85(7-8), 437-445..

[8] Bathe K. J., Noh, G. (2012). Insight into an implicit time integration scheme for structural dynamics. *Computers & Structures*, 98, 1-6.

[9] Hulbert, G. M. (2010). Limitations on linear multistep methods for structural dynamics. *Earthquake Engineering & Structural Dynamics*, 20(2), 191-196.

[10] Hughes, T. J. R. (1983). Analysis of transient algorithms with particular reference to stability behavior, in T. Belytschko and T. J. R. Hughes (eds.), Computational Methods for Transient Analysis. *North-Holland, Amsterdam*, 67-155.

[11] Hinton, E., Rock, T., & Zienkiewicz, O. C. (1976). A note on mass lumping and related processes in the finite element method. Earthquake Engineering & Structural Dynamics, 4(3), 245-249.

[12] Hilber H. M. (1976).Analysis and design of numerical integration methods in structural dynamics. EERC Report No. 76-29, *Earthquake Engineering Research Center*, *University of California*, Berkeley, CA.

[13] Huang, Y., Sturt, R., & Willford, M. (2019). A damping model for nonlinear dynamic analysis providing uniform damping over a frequency range. Computers & Structures, 212, 101-109.